*Int. J. Electrochem. Sci.*, 15 **(2020)** 8181 – 8189, doi: 10.20964/2020.08.69

International Journal of
ELECTROCHEMICAL
SCIENCE
www.electrochemsci.org

# A Facile synthesis of the Nickel Oxide Nanoparticles for the Effective Electrochemical Detection of Hydrogen peroxide in Contact Lens Solution

*Praveen Kumar G*[1] *,Selvarasu Maheshwaran*[1]*, Shen-Ming Chen*[1,*]*, Muthumariappan Akilarasan*[1] *, Tse-Wei Chen*[2,3,4]*, Tien-Wen Tseng*[2,*]*, Jaysan Yu*[4]*, Richard Yu*[4]*,*

[1] Electroanalysis and Bioelectrochemistry Lab, Department of Chemical Engineering and Biotechnology, National Taipei University of Technology, Taipei, Taiwan 106 (ROC).
[2] Department of Chemical Engineering and Biotechnology, National Taipei University of Technology, Taipei 10608, Taiwan, ROC
[3] Research and Development Center for Smart Textile Technology, National Taipei University of Technology, Taipei 106, Taiwan, ROC.
[4] Well Fore special wire corporation, 10, Tzu-Chiang 7 rd., Chung-Li Industrial Park, Taoyuan, Taiwan
[*]E-mail: smchen78@ms15.hinet.net, f10403@ntut.edu.tw

*Received:* 6 May 2020 / *Accepted:* 10 June 2020 / *Published:* 10 July 2020

Hydrogen peroxide ($H_2O_2$) was secreted in the mitochondria during the cell production. Moreover, $H_2O_2$ was act as a key member for reactive oxidative species. The imbalance of reactive oxidative species causes various health risks. Therefore, it is important to develop a device to detect $H_2O_2$. Thus, nickel oxide nanoparticles (NiO NPs) were synthesized using the simple co-precipitation method for the detection of $H_2O_2$. The morphological and chemical composition of the as prepared NiO NPs was characterized by using FESEM and XRD. Herein, we reported that the synthesized NiO NPs modified GCE shows a selective detection towards the $H_2O_2$. Moreover, the NiO NPs/GCE has displayed wider covering range of 8.6 nM to 433.24µM with the detection limit up to 4.28nM. The NiO NPs/GCE has successfully examined with contact lens cleaning solution for the practical application for detection of $H_2O_2$, which shows the appreciable found and recovery.

**Keyword:** Nickel oxide; $H_2O_2$ sensor; reactive oxidative species; electrochemical method; contact lens cleaning solution.

## 1. INTRODUCTION

Hydrogen peroxide ($H_2O_2$) has been widely used in biological and pharmaceutical industrial applications. Furthermore, $H_2O_2$ acts a key member for the production of reactive oxygen species[1]. Moreover, the $H_2O_2$ has been produced naturally in the living cell at the mitochondria, which regulates

the cell productions. Over secretion of $H_2O_2$ will leads to aging and several neurotransmitter diseases[2]. Therefore, it is essential to develop a cost-effective and eco-friendly device for determination of $H_2O_2$. In recent, there are various techniques are used to monitoring the $H_2O_2$ level. However, electrochemical techniques are simple, rapid, easy to handle and cost effective[3]. While using the enzymatic sensors encounters various issues such as instability, easily affected by the environment, lack of durability and complicated immobilization procedures[4]. To overcome this, recently researcher had much interested to develop the non-enzymatic sensor based on the metal oxides[5].

In recent nanostructured, metal oxides have been widely used in the field of electrochemical sensors, supercapacitors, and solar cell applications[6]. Generally, transition metal oxides have been investigated more in the field of electrochemical sensor compare with rare earth metal oxide[7, 8]. However, the rare earth metals have some unique properties such as providing larger surface area, less size, and interfacial effects[9]. Among them NiO is a P-type semiconductor, so it has a wide range of electrochemical application[10]. Furthermore, the nickel oxide holds the wide range band gap of 3.6 - 4.0 eV and significant refractive index of 1.93 [11, 12]. Thus, considering the unique properties of NiO we have developed the electrochemical sensor based on it.

Herein, we reported the effective electrochemical sensor based on the NiO NPs for the $H_2O_2$ sensing. The NiO NPs modified nanomaterials shows the charger transfer resistance of $R_{ct}$ of the 105.02 Ω. Furthermore, the NiO NPs/GCE significantly enhanced the detection of $H_2O_2$, the as prepared sensor shows the remarkable performance in the real sample such as contact lens cleaning solution.

## 2. MATERIALS AND METHODS

Nickel nitrate hexahydrate ($Ni(NO_3)_2.6H_2O$) and Sodium hydroxide (NaOH), potassium hydroxide (KOH), hydrogen peroxide solution ($H_2O_2$), D (+)-glucose, L-ascorbic acid, folic acid, dopamine hydrochloride, uric acid and 3-Nitro-L-tyrosine were obtained from sigma-Aldrich and used without any further purification. Double distilled water was used for all the experiments. 0.1 M KOH was used as supporting electrolyte. Contact lens cleaning solutions were purchased from local pharmacy in Taipei city, Taiwan.

The surface modification of the as-formed composite was probed using field emission scanning electron microscope (FESEM-JEOL-7600F). PerkinElmer PHI-5702 investigated the quantitative analysis, defects, and disorder nature of the as-prepared composite and the XRD, XPERT-PRO spectrometer (PANalytical B.V.) was used to observe the crystallinity nature and purity of the composite. The electrochemical property and electrocatalytic activity were scrutinized using electrochemical impedance spectroscopy (EIS), cyclic voltammetry (CV), and it-Amperometry were carried out using CHI 1205A. The CHI instrument consists of three electrodes system, whereas, the platinum wire and Ag/AgCl (sat. KCl) were used as an auxiliary and reference electrode and pre-washed GCE (glassy carbon electrode) act as a working electrode.

## 3. EXPERIMENTAL SECTION

### *3.1. Synthesis of NiO nanoparticles*

The NiO NPs were synthesized using simple co-precipitation method. 0.5M of $Ni(NO_3)_2 .6H_2O$ was dissolved in 50 ml of distilled water and to the solution 1M NaOH were added slowly with vigorous stirring. The obtained precipitate was centrifuged and washed with water for several time to remove the $Na^+$ ions and calcinated at $400^0$ C for 2 h[13].

### *3.2. Preparation of NiO NPs modified GCE*

The GCE surface was polished three repeated times with 0.5mg of $Al_2O_3$ slurry. Then, 1mg of synthesized NiO NPs was dispersed in 1 ml of ethanol and sonicated for 15 min. Finally, the 6µL of NiO NPs colloidal were drop-coated on the polished GCE surface and dried at $50^0$ C. The prepared NiO NPs/GCE was used for further electrochemical analysis.

## 4. RESULTS AND DISCUSSION

### *4.1. FESEM and XRD NiO NPs*

The morphological structure of the synthesized nanomaterials was explored using FE-SEM. Fig. 1A-B displays the FESEM image of the NiO NPs with different magnification. In Fig.1A, particles are slightly agglomerates and arranged irregular shape. Further, the magnified FESEM image of the NiO NPs clearly shows that numerous particles are in sphere like structure as displayed in Fig.1B.

The synthesized NiO XRD pattern were displayed in Fig.1C it shows the characteristic peaks at $37.24^0$(111), $43.27^0$(200), $62.88^0$(220), $75.41^0$(311), $79.40^0$(222). The obtained peaks were agreeing with the standard XRD of NiO (JCPDS No. 047-1049)[14]. The synthesized NiO belongs to the cubic crystal system. The crystalline size of the synthesized NiO and found to be 9.27nm using the Scherrer equation (1)[15].

$$D = (k\lambda/\beta \cos \theta) \quad \textbf{(1)}$$

Were D is the crystalline size of the particle(nm), k is the dimensionless shape factor (0.94), λ is the wavelength of X-Ray (1.54178Å), β was the Full width at half maximum of the diffraction peak (FWHW) and θ is the diffraction angle.

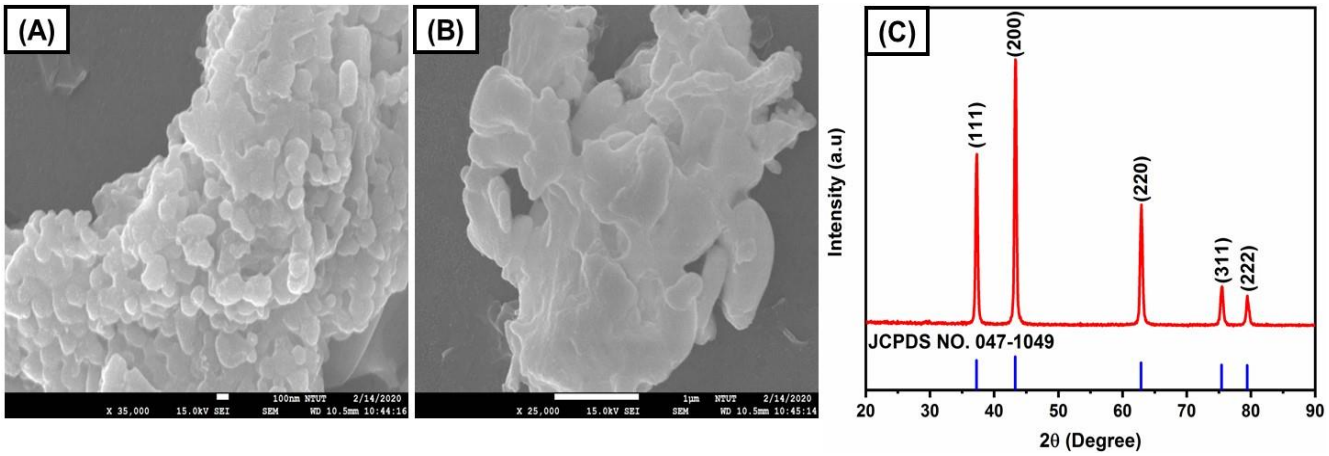


**Figure 1.** FE-SEM of NiO NPs (A-B) XRD spectrum of NiO (C)

*4.2. EIS and Electrochemical study of different electrodes*

The EIS spectrum for the bare GCE (a) and NiO NPs/GCE (b) were performed with the frequency range of 100MHz to 100KHz using 0.1M KCl containing 0.05M $[Fe(CN)_6]^{3-/4-}$ were shown on Fig.2A. The EIS Spectrum was fitted according to the Randle's equivalent circuit model displayed on inset Fig.2A were $R_{ct}$, $Z_w$, $R_s$ and $C_{dl}$ are charge transfer resistance, Warburg impedance, ohmic resistance and the double layer electron-transfer resistance. Further, the larger semicircle portion with the higher frequency obtained for the bare GCE and the $R_{ct}$ value was measured to be 182.32 Ω. Moreover, the smaller semicircle region with the lower frequency obtained at NiO NPs/GCE and it $R_{ct}$ value was calculated to be 105.02 Ω. Thus, the conductivity between the GCE surface and the electrolyte was improved by NiO modified electrode.

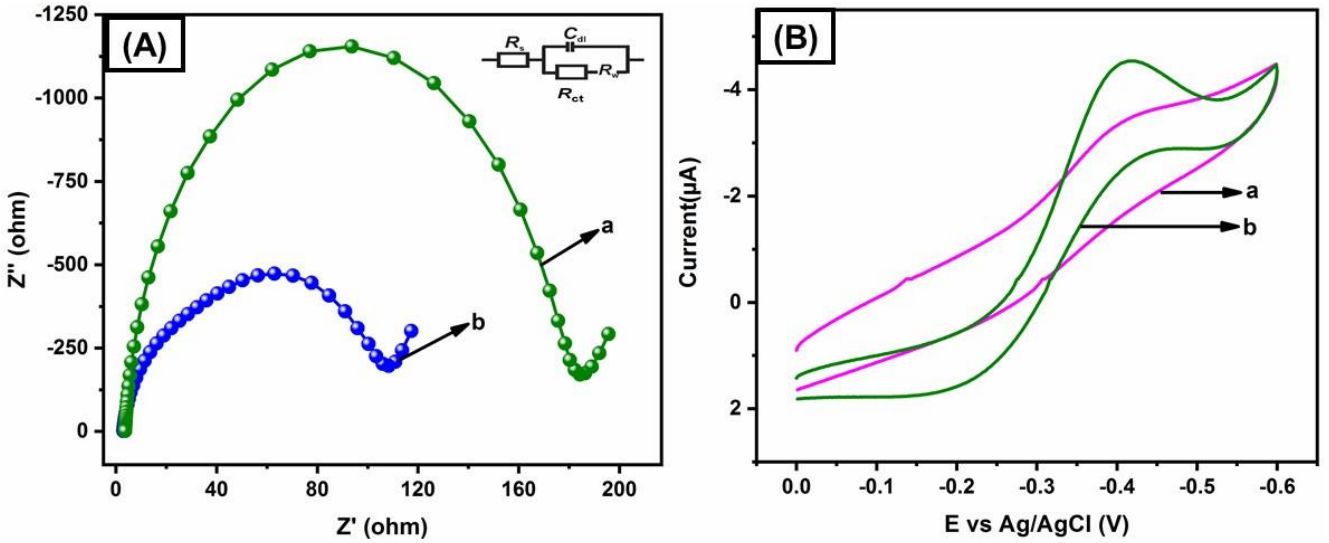


**Figure 2.** (A) EIS of bare GCE (a) and NiO NPs/GCE (b) in 0.1 M KOH 0.05M $[Fe(CN)_6]^{3-/4-}$. (B) CV's of bare GCE (a) and NiO NPs/GCE (b) in presence of 50μM $H_2O_2$ at 0.1 M KOH

The CV curve response for bare GCE (a) and NiO NPs/GCE (b) at 0.1 M KOH containing 50μM of $H_2O_2$ with fixed scan rate of 0.05V/s was shown on Fig.2B. NiO NPs/GCE shows excellent cathodic

peak current of -4.54µA at lower reduction potential of -0.41 V comparing to the bare GCE. This confirms that NiO NPs fabricated GCE shows excellent sensitivity towards the detection of $H_2O_2$.

### *4.3. Influence of concentration and scan rate on NiO NPs/GCE*

The influence of $H_2O_2$ concentration were examined by varying the concentration from 25µM to 200µM with a constant scan rate of 0.05V/s were displayed on Fig.3A. The cathodic peak current increased linearly with every consecutive addition of $H_2O_2$. Additionally, the correlation between cathodic current vs $H_2O_2$ concentration has shown on Fig.3B. The regression equation for cathodic current was written as y= -0.03195x -3.1723 with correlation coefficient of $R^2$=0.9930. Fig.3C shows the different scan rate curve ranging from 0.02 to 0.2V/s for NiO NPs/GCE in 0.1M KOH consist of 100µM of $H_2O_2$. The cathodic current increase linearly with increase in scan rate. Fig.3D shows the cathodic peak current obtained for $H_2O_2$ vs $(Scanrate)^{1/2}(Vs^{-1})^{1/2}$. The regression equation for reduction peak was written as y = -12.139x - 3.3237 with correlation coefficient of $R^2$ = 0.9979, which shows that reduction of $H_2O_2$ by NiO NPs/GCE was diffusion-controlled process[16].

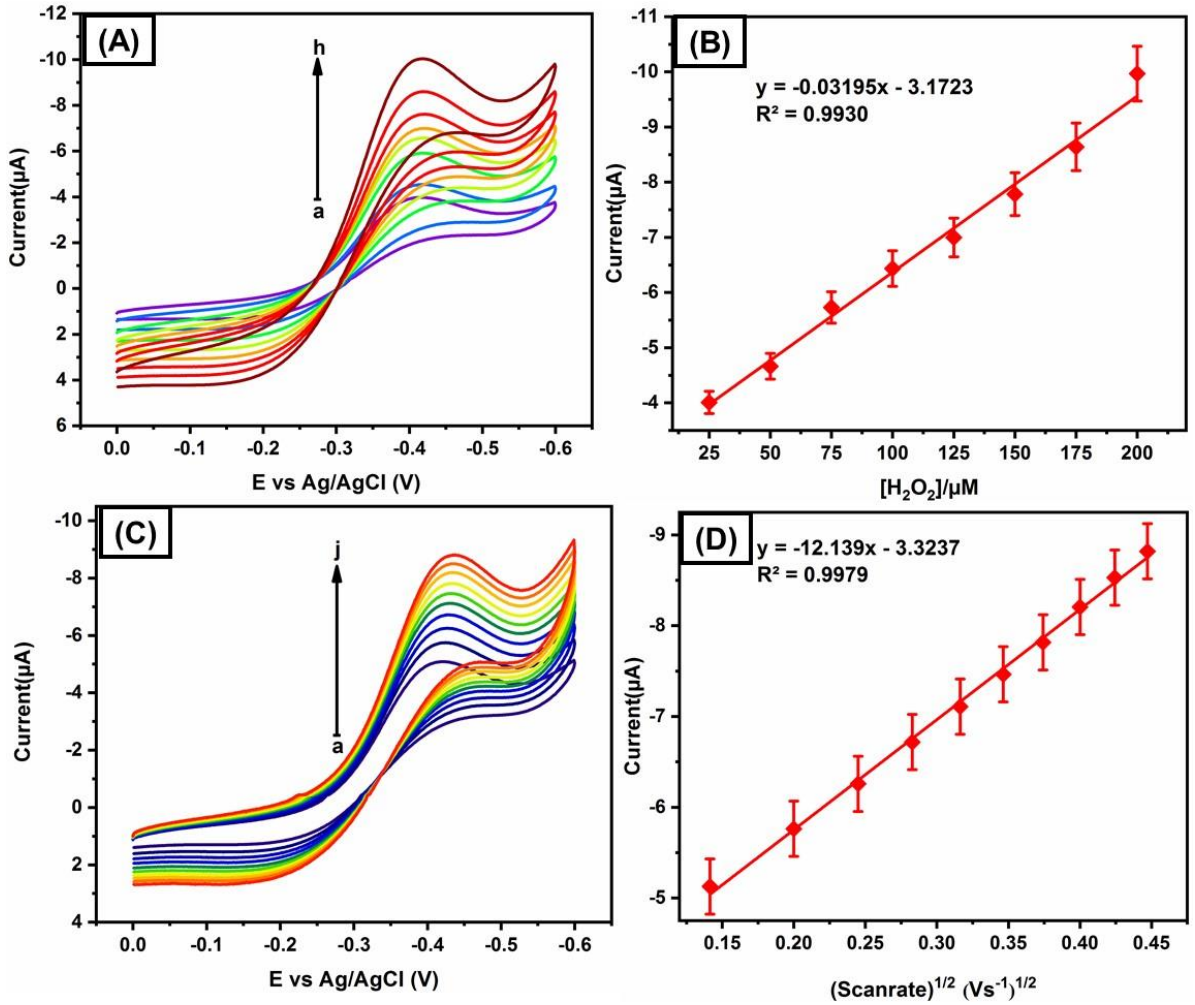


**Figure 3.** Effect of concentration 20 to 200µM $H_2O_2$ on NiO NPs/GCE (A) and CVs occurred for NiO NPs/GCE at increasing scan rates (0.02 to 0.2 $Vs^{-1}$) (C) in 0.1 M KOH containing 100µM $H_2O_2$. Linear plot for redox current peak Vs DA concentration (B) and square root of scan rate (D).

*4.4. Amperometric detection of $H_2O_2$ using NiO NPs modified GCE*

Fig.4A shows the it-Amperometric response of the NiO NPs/GCE towards sequential addition of $H_2O_2$ in 0.1M KOH with the applied potential of -0.35 V with 1200 rotation per minute. For every addition of $H_2O_2$ linear increase of current has observed and the responsive current reach get stabilized within 5s. Fig.4B displays the current versus $H_2O_2$ concentration and the linear regression equation was found to be $I_{pc}/\mu M = 0.0824[H_2O_2]/\mu M + 0.0479$. The linear range for the working concentration was 8.6nM to 433.24 µM with the limit of detection (LOD) 4.28 nM. The LOD was determined using the formula, $LOD = 3\sigma s_b/S$ where $s_b$ was the standard deviation of 20 blank measurement and S is the sensitivity. So, the developed NiO NPs/GCE shows an excellent sensitivity towards the $H_2O_2$ compared to previously reported literature (Table-1).

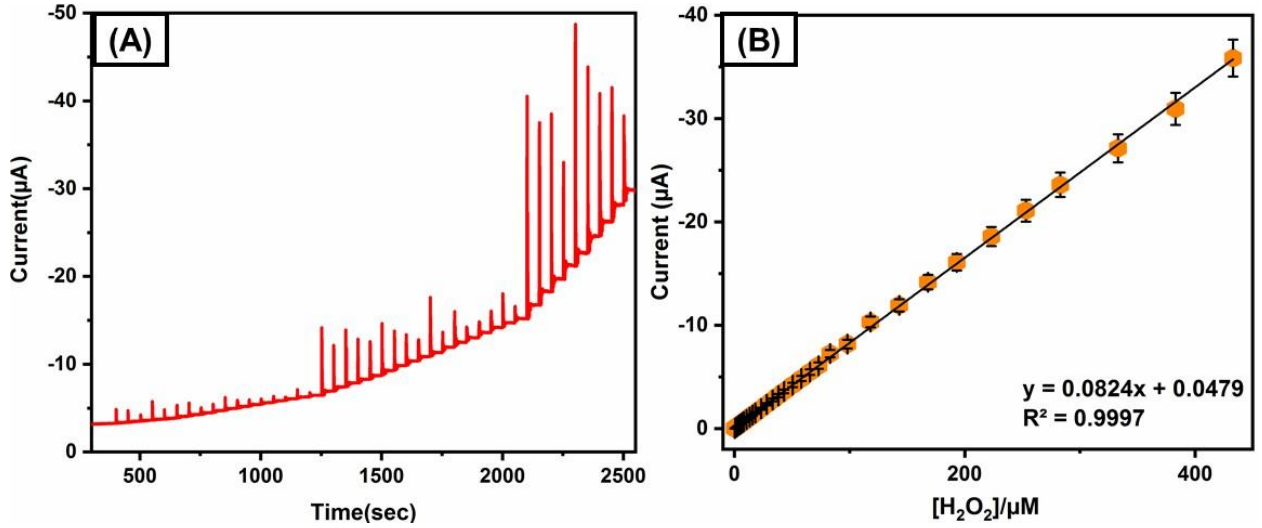


**Figure 4.** (A) it-Amperometry response for the increase in concentration of $H_2O_2$ in 0.1 M KOH with respect to NiO NPs/GCE. (B) Linear plot of anodic peak current Vs $H_2O_2$[µM].

*4.5. Interference and Stability of the NiO NPs/GCE*

The selectivity and stability are the two vital elements for the electrochemical sensor. The it-Amperometry study was performed to confirm the selectivity of NiO NPs/GCE towards $H_2O_2$ detection. The selectivity was performed in presence of 5 fold of higher possible interferons like dopamine (DA), uric acid (UA), glucose (Glu), folic acid (FA), ascorbic acid (AA), 3 nitro-l-tyrosine (3NT) were given in Fig.5A it clearly shows that the NiO NPS modified GCE exhibit a particular selectivity towards the $H_2O_2$ sensing. The working stability of the NiO NPs/GCE were performed in the presence of 0.1M KOH consist of 100µM of $H_2O_2$ for 15 days and the electrode was stored under $4^0$ C after every use was shown in Fig.5B The electrode showed 93.04% of its initial current response. It shows that synthesized NiO NPs modified electrode shows an excellent stability towards the $H_2O_2$ detection.

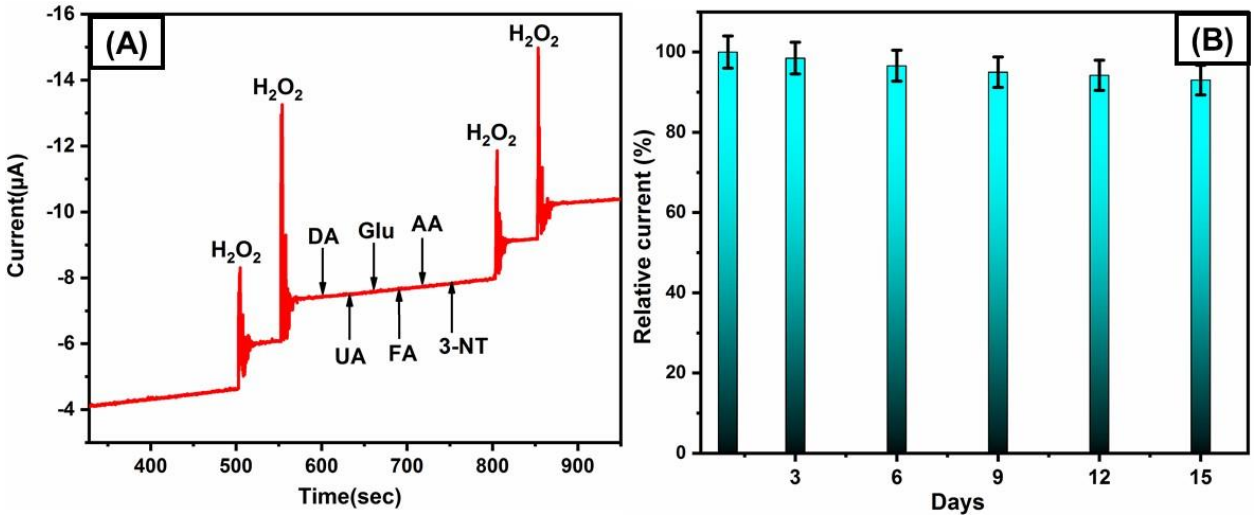


**Figure 5.** (A) Selective responses of NiO NPs/GCE towards $H_2O_2$ using it-amperometry technique. (B) Stability of NiO NPs/GCE for continuous usage for 15 days towards 100μM of $H_2O_2$ in 0.1M KOH.

**Table 1.** Comparative studies of $H_2O_2$ detection by NiO NPs/GCE with different electrodes from the earlier reports

| Electrodes | Linear range (μM) | Limit of Detection (μM) | Reference |
|---|---|---|---|
| [a]Fe-NGCs/[b]it-amp | 1-5000 | 0.53 | [17] |
| [c]AgNPs/CQDs/[b]it-amp | 0.2-27.0 | 0.08 | [18] |
| [d]HRP/LDH-CMC/[b]it-amp | 20.6000 | 12.4 | [19] |
| [e]Ag-mSiO2/[b]it-amp | 4-10000 | 3 | [20] |
| [f]AuNPs-NH2/Cu MOF/[b]it-amp | 5–850 | 1.2 | [21] |
| [g]H-ERGo/GCE/[b]it-amp | 25–8850; 8850–28850 | 8.33 | [22] |
| NiO NPs/GCE | 8.6nM to 433.24 μM | 0.00428 | **This work** |

[a]-M-Nx (M = Fe, Co, Ni, Cu) doped graphitic nano cages.
[b]- it-Amperometry
[c]-Silver nanoparticles/ carbon quantum dots.
[d]-Chitosan/2D layered double hydroxide-carboxymethyl chitosan.
[e]-Silver Doped Mesoporous Silica Nanoparticles.
[f]-Ammoniated- Au nanoparticles/ Cu-based metalorganic framework modified glassy carbon electrode.
[g]-Facile Preparation of Hemin-functionalized Reduced Graphene Oxide Nanocomposite/ Glassy carbon electrode.

*4.6. Real sample analysis of NiO NPs/GCE*

The practical application for the NiO NPs/GCE was tested using the it-Amperometric technique. Thus, the practical applicability of the of the prepared the sensor was tested in the contact lens cleaning

solution. However, these solutions already contained inherent $H_2O_2$ and hence directly spiked into the supporting electrode and amperometry experiments were performed by following the optimized experimental conditions of lab samples. As the results, NiO NPs/GCE provide the owing found and recovery values, which are tabulated in **table.2**. In the end, the prepared NiO NPs/GCE established as an effective electrode for the practical application.

**Table 2.** Real sample analysis of $H_2O_2$ in spiked contact lens cleaning solution on NiO NPs/GCE

| Real Samples | Added/nM | Found/nM | Recovery/% | *RSD/% (n=3) |
|---|---|---|---|---|
| Contact lens cleaning solution | 50 | 50 | 100.84 | ±2.18 |
| | 100 | 103 | 102.65 | ±2.42 |
| | 200 | 201 | 100.57 | ±1.69 |

* Related standard deviation (RSD).

## 5. CONCLUSION

In summary, NiO NPs were successively prepared using the simple chemical co-precipitation method and its morphology and purity were confirmed using FE-SEM and XRD Studies. Further, NiO NPs fabricated GCE owing an excellent electrochemical response towards the detection of $H_2O_2$. Moreover, the proposed NiO NPs/GCE shows a linear range of 8.6nM to 433.24 µM with the detection of limit 4.28 nM. Additionally, the NiO NPs/GCE exhibit the higher selectivity and excellent stability towards the $H_2O_2$ detection. Further, the practical application were performed using the contact lens cleaning solution, which shows the good recovery. To our knowledge, the as synthesized NiO NPs is one of the most effective electrocatalyst for the detection of $H_2O_2$.

CONFLICT OF INTEREST

The authors declare that there is no Conflict of interest.

ACKNOWLEDGMENTS

This project was supported by the Ministry of Science and Technology (MOST 107-2113-M-027 -005 -MY3), Taiwan (ROC).

## References

1. S. Kogularasu, M. Govindasamy, S.-M. Chen, M. Akilarasan, V. Mani, *Sens. Actuators, B: Chem.*, 253 (2017) 773-783.
2. K. Sakthivel, G. Mani, S.-M. Chen, S.-H. Lin, A. Muthumariappan, V. Mani, *J. Electroanal. Chem.*, 820 (2018) 161-167.
3. E. Tamilalagan, M. Akilarasan, S.-M. Chen, T.-W. Chen, Y.C. Huang, Q. Hao, W. Lei, *Ultrason. Sonochem.*, (2020) 105164.
4. Y. Sun, K. He, Z. Zhang, A. Zhou, H. Duan, *Biosens. Bioelectron.*, 68 (2015) 358-364.

5. A.A. Ensafi, M.M. Abarghoui, B. Rezaei, *Electrochim. Acta*, 190 (2016) 199-207.
6. V. Sudha, S.M.S. Kumar, R. Thangamuthu, *J. Alloys Compd.*, 744 (2018) 621-628.
7. Y. Xi, D. Li, A. Djurišić, M. Xie, K. Man, W. Chan, *Electrochem. Solid-State Lett.*, 11 (2008) D56-D59.
8. S. Kogularasu, M. Akilarasan, S.-M. Chen, T.-W. Chen, B.-S. Lou, *Mater. Chem. Phys.*, 227 (2019) 5-11.
9. R. Umamaheswari, M. Akilarasan, S.-M. Chen, Y.-H. Cheng, V. Mani, S. Kogularasu, F.M. Al-Hemaid, M.A. Ali, X. Liu, *J. Colloid Interface Sci.*, 505 (2017) 1193-1201.
10. C. Yuan, X. Zhang, L. Su, B. Gao, L. Shen, *J. Mater. Chem.*, 19 (2009) 5772-5777.
11. C.A. Niedermeier, M. Råsander, S. Rhode, V. Kachkanov, B. Zou, N. Alford, M.A. Moram, *Sci. Rep.*, 6 (2016) 31230.
12. J. Hugel, C. Carabatos, *J. Phys. C: Solid State Phys.*, 16 (1983) 6713.
13. M.-S. Wu, H.-H. Hsieh, *Electrochim. Acta*, 53 (2008) 3427-3435.
14. H. Xu, M. Zeng, J. Li, X. Tong, *RSC Adv.*, 5 (2015) 91493-91499.
15. A. Monshi, M.R. Foroughi, M.R. Monshi, *WJNSE*, 2 (2012) 154-160.
16. A. Muthumariappan, K. Sakthivel, S.-M. Chen, T.-W. Chen, A.M. Elgorban, M.S. Elshikh, N. Marraiki, *New J. Chem*, 44 (2020) 605-613.
17. Z.M. Sheng, H. Huang, R.L. Niu, Z.W. Han, R.P. Jia, *Sens. Actuators, B: Chem.*, 305 (2020) 127550.
18. M. Jahanbakhshi, B. Habibi, *Biosens. Bioelectron.*, 81 (2016) 143-150.
19. J. Yuan, S. Xu, H.-Y. Zeng, X. Cao, A.D. Pan, G.-F. Xiao, P.-X. Ding, *Bioelectrochem.*, 123 (2018) 94-102.
20. D. Yang, N. Ni, L. Cao, X. Song, Y. Alhamoud, G. Yu, J. Zhao, H. Zhou, *Micromachines*, 10 (2019) 268.
21. W. Dang, Y. Sun, H. Jiao, L. Xu, M. Lin, *J. Electroanal. Chem.*, 856 (2020) 113592.
22. Z. Chen, D. Liu, C. Zhu, L. Li, T. You, *Sens. Mater.*, 31 (2019) 1167-1179

© 2020 The Authors. Published by ESG (www.electrochemsci.org). This article is an open access article distributed under the terms and conditions of the Creative Commons Attribution license (http://creativecommons.org/licenses/by/4.0/).